

Coordination Polymers from Silver(I) and Bifunctional Pyridyl Ligands

Moonhyun Oh, Charlotte L. Stern, and Chad A. Mirkin*

Department of Chemistry and the Center for Nanofabrication and Molecular Self-Assembly,
Northwestern University, Evanston, Illinois 60208-3113

Received December 3, 2004

Coordination polymers and a macrocycle formed from the reactions between flexible bis(2-pyridyl) ligands and AgCF_3SO_3 are reported. The type of structure formed depends on the choice of ligand and the stoichiometry of the reaction. When 1 equiv of 1,4-bis(pyridin-2-ylmethoxy)benzene (L2), 4,4'-bis(pyridin-2-ylmethoxy)biphenyl (L4), or bis((4-pyridin-2-ylmethoxy)phenyl)methane (L5) is used, 1D chain coordination polymers held together via Ag–N bonds are generated. When a 2:1 ratio of L2 and silver ion is used, a 2D porous network is formed. The reaction between silver ions with a mixture of ligands (L1 and L2 in 1:1 ratio, L1 = 1,4-bis((pyridin-2-yl-methyl)thio)benzene) results in a novel 1D ABAB type coordination copolymer where L1 and L2 act as a bis-bidentate and a bis-monodentate ligand, respectively. The reaction of 1-(pyridin-2-ylmethoxy)-4-((pyridin-2-yl-methyl)thio)benzene (L3) with silver ions in a 1:1 ratio gives a bimetallic macrocycle rather than a polymeric species. Structural analyses of the polymeric compounds suggest that interactions between the aromatic rings play a significant role in stabilizing the polymeric structures.

Introduction

Although there are now a variety of well-characterized metal–ligand coordination polymers,^{1,2} there are very few methods that allow one to design different types of structures with control over chemical linkage and internal pore structure. Such control could allow one to design polymer architectures with unusual and potentially useful catalytic, recognition, and sieving properties.² The structures of such polymeric species are determined by several factors, including the coordination environment of the metal nodes, the type of ligands used to connect the metal nodes, and noncovalent interactions such as hydrogen bonds and aromatic–aromatic interactions that can help stabilize certain architectures.^{1–5} Over the past few years, numerous coordination polymers and macrocycles have been generated from

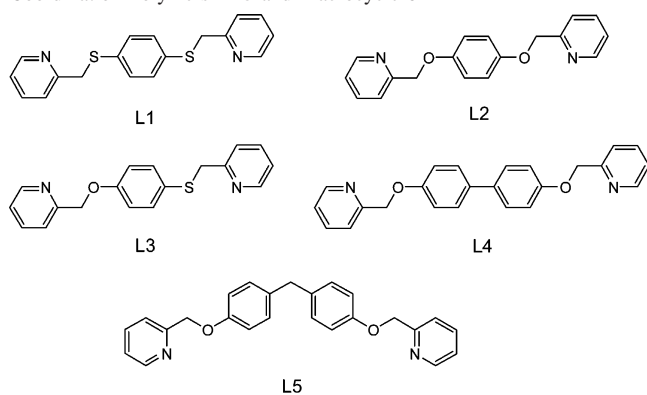
transition metal nodes with rigid and flexible pyridyl-containing bidentate or multidentate organic spacers.^{6,7} Despite these advances, there is not a good understanding of how metal–ligand stoichiometry can be used to control the type of polymeric structures that ultimately form in these reactions.⁸ Herein, we report a study that focuses on evaluating the types of polymeric and macrocyclic structures

* Author to whom correspondence should be addressed. E-mail: chadnano@northwestern.edu.

- (1) (a) Moulton, B.; Zaworotko, M. J. *Chem. Rev.* **2001**, *101*, 1629. (b) Robson, R. J. *Chem. Soc., Dalton Trans.* **2000**, 3735. (c) Oh, M.; Carpenter, G. B.; Sweigart, D. A. *Acc. Chem. Res.* **2004**, *37*, 1. (d) Philp, D.; Stoddart, J. F. *Angew. Chem., Int. Ed. Engl.* **1996**, *35*, 1154. (e) Eddaoudi, M.; Moler, D. B.; Li, H.; Chen, B.; Reineke, T. M.; O'Keeffe, M.; Yaghi, O. M. *Acc. Chem. Res.* **2001**, *34*, 319. (f) Desiraju, G. R. *Nature* **2001**, *412*, 397.
- (2) (a) Evans, O. R.; Lin, W. *Acc. Chem. Res.* **2002**, *35*, 511. (b) Kitagawa, S.; Kitaura, R.; Noro, S.-i. *Angew. Chem., Int. Ed.* **2004**, *43*, 2334. (c) Chen, B.; Eddaoudi, M.; Hyde, S. T.; O'Keeffe, M.; Yaghi, O. M. *Science* **2001**, *291*, 1021. (d) Tabellion, F. M.; Seidel, S. R.; Arif, A. M.; Stang, P. J. *Angew. Chem., Int. Ed.* **2001**, *40*, 1529. (e) Kasai, K.; Aoyagi, M.; Fujita, M. *J. Am. Chem. Soc.* **2000**, *122*, 2140.

- (3) (a) Braga, D.; Grepioni, F. *J. Chem. Soc., Dalton Trans.* **1999**, 1. (b) Allen, M. T.; Burrows, A. D.; Mahon, M. F. *J. Chem. Soc., Dalton Trans.* **1999**, 215. (c) Oh, M.; Carpenter, G. B.; Sweigart, D. A. *Organometallics* **2002**, *21*, 1290. (d) Ziener, U.; Breuning, E.; Lehn, J.-M.; Wegelius, E.; Rissanen, K.; Baum, G.; Fenske, D.; Vaughan, G. *Chem.—Eur. J.* **2000**, *6*, 4132. (e) Parker, R. J.; Spiccia, L.; Batten, S. R.; Cashion, J. D.; Fallon, G. D. *Inorg. Chem.* **2001**, *40*, 4696. (f) Fraser, C. S. A.; Jenkins, H. A.; Jennings, M. C.; Puddephatt, R. J. *Organometallics* **2000**, *19*, 1635–1642. (g) Steiner, T. *Angew. Chem., Int. Ed.* **2002**, *41*, 48.
- (4) (a) Roesky, H. W.; Andruh, M. *Coord. Chem. Rev.* **2003**, *236*, 91. (b) Reger, D. L.; Semeniuc, R. F.; Rassolov, V.; Smith, M. D. *Inorg. Chem.* **2004**, *43*, 537. (c) Hunter, C. A.; Sanders, J. K. M. *J. Am. Chem. Soc.* **1990**, *112*, 5525. (d) Janiak, C. *J. Chem. Soc., Dalton Trans.* **2000**, 3885. (e) Chand, B.; Ray, U.; Mostafa, G.; Lu, T.-H.; Sinha, C. *Polyhedron* **2004**, *23*, 1669. (f) Aravinda, S.; Shamala, N.; Das, C.; Sriranjini, A.; Karle, I. L. Balaram, P. *J. Am. Chem. Soc.* **2003**, *125*, 5308.
- (5) (a) Jennings, W. B.; Farrell, B. M.; Malone, J. F. *Acc. Chem. Res.* **2001**, *34*, 885. (b) Nishio, M. *CrystEngComm* **2004**, *6*, 130. (c) Kobayashi, K.; Ishii, K.; Sakamoto, S.; Shirasaka, T.; Yamaguchi, K. *J. Am. Chem. Soc.* **2003**, *125*, 10615. (d) Zhao, R.; Matsumoto, S.; Akazome, M.; Ogura, K. *Tetrahedron* **2002**, *58*, 10233. (e) Sénéque, O.; Giorgi, M.; Reinaud, O. *Chem. Commun.* **2001**, 984. (f) Takahashi, H.; Tsuboyama, S.; Umezawa, Y.; Honda, K.; Nishio, M. *Tetrahedron* **2000**, *56*, 6185.

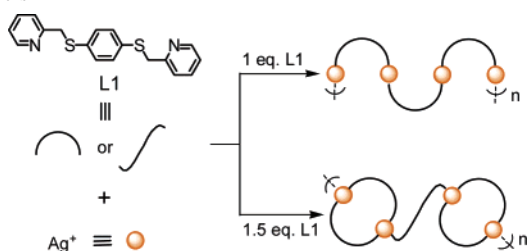
Chart 1. Flexible Pyridyl-Type Ligands Used To Synthesize Coordination Polymers 1–5 and Macrocycle 6



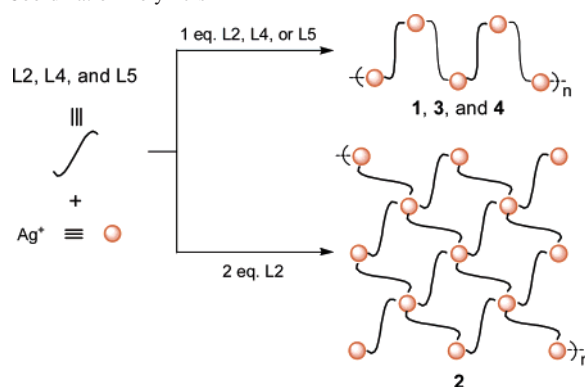
that form as a function of ligand type and metal–ligand stoichiometry in the context of a class of bipyridyl ligands with different types of chemical spacers. This work builds off of the efforts of supramolecular coordination chemists to use coordination chemistry principles and ligand design to tailor resulting molecular architecture.^{1–9}

For our studies, we have synthesized several new bis(2-pyridyl) ligands, 1-(pyridin-2-ylmethoxy)-4-((pyridin-2-ylmethyl)thio)benzene (L3), 4,4'-bis((pyridin-2-ylmethoxy)thio)biphenyl (L4), and bis((4-pyridin-2-ylmethoxy)phenyl)methane (L5), as well as two previously reported ligands, 1,4-bis((pyridin-2-ylmethyl)thio)benzene (L1)¹⁰ and 1,4-bis((pyridin-2-ylmethoxy)thio)benzene (L2)¹¹ (Chart 1), and investigated their reactivity with silver ions. In previous work,¹⁰ we reported that silver metal ions and L1 react to cleanly generate two types of polymers, depending upon the ratio of starting materials used. In one case, ligand L1 adopts a

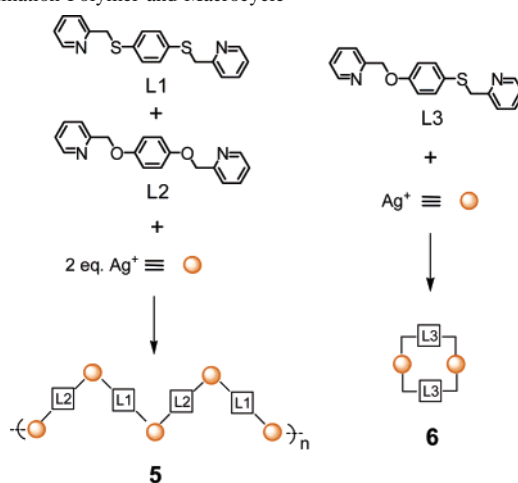
Scheme 1. Stoichiometric Control in the Synthesis of Coordination Polymers



Scheme 2. Schematic Representation for the Stoichiometric Control of Coordination Polymers



Scheme 3. Schematic Representation for the Formation of Coordination Polymer and Macrocycle



folded conformation to yield a 1D zigzag polymer, and in the second example, the ligand adopts both linear and folded conformations within the structure, producing a novel coordination polymer with macrocyclic cages confined within its backbone (Scheme 1).

In this study, we report the synthesis and characterization of the novel coordination polymers, {[Ag(L2)]CF₃SO₃}_n (**1**), {[Ag(L2)₂]CF₃SO₃}_n (**2**), {[Ag(L4)]CF₃SO₃}_n (**3**), {[Ag(L5)]-CF₃SO₃}_n (**4**), {[Ag₂(L1)(L2)]·2CF₃SO₃}_n (**5**), and a macrocycle [Ag(L3)]₂·2CF₃SO₃ (**6**), derived from the reactions of AgCF₃SO₃ with ligands L1–L5 (Schemes 2 and 3). Significantly, polymer **5** is a rare example of a coordination copolymer¹² generated from the combination of two different organic ligands functionalized with two similar 2-pyridyl

- (6) (a) Khlobystov, A. N.; Blake, A. J.; Champness, N. R.; Lemenovskii, D. A.; Majouga, A. G.; Zyk, N. V.; Schröder, M. *Coord. Chem. Rev.* **2001**, *222*, 155. (b) Burchell, T. J.; Eisler, D. J.; Puddephatt, R. J. *Chem. Commun.* **2004**, 944. (c) Shin, D. M.; Lee, I. S.; Lee, Y.-A.; Chung, Y. K. *Inorg. Chem.* **2003**, *42*, 2977. (d) Zhu, H.-F.; Kong, L.-Y.; Okamura, T.-a.; Fan, J.; Sun, W.-Y.; Ueyama, N. *Eur. J. Inorg. Chem.* **2004**, 1465. (e) Horikoshi, R.; Mochida, T.; Maki, N.; Yamada, S.; Moriyama, H. *J. Chem. Soc., Dalton Trans.* **2002**, 28. (f) Caradoc-Davies, P. L.; Hanton, L. R.; Henderson, W. *J. Chem. Soc., Dalton Trans.* **2001**, 2749. (g) Caradoc-Davies, P. L.; Hanton, L. R. *Chem. Soc., Dalton Trans.* **2003**, 1754. (h) Carlucci, L.; Ciani, G.; Proserpio, D. M.; Porta, F. *Angew. Chem., Int. Ed.* **2003**, *42*, 317. (i) Tong, M.-L.; Wu, Y.-M.; Ru, J.; Chen, X.-M.; Chang, H.-C.; Kitagawa, S. *Inorg. Chem.* **2002**, *41*, 4846.
- (7) (a) Ohi, H.; Tachi, Y.; Itoh, S. *Inorg. Chem.* **2004**, *43*, 4561. (b) Shin, D. M.; Lee, I. S.; Cho, D.; Chung, Y. K. *Inorg. Chem.* **2003**, *42*, 7722. (c) Caradoc-Davies, P. L.; Hanton, L. R.; Hodgkiss, J. M.; Spicer, M. D. *J. Chem. Soc., Dalton Trans.* **2002**, 1581. (d) Schneider, R.; Hosseini, M. W.; Planeix, J.-M.; Cian, A. D.; Fischer, J. *Chem. Commun.* **1998**, 1625.
- (8) (a) Cotton, F. A.; Lin, C.; Murillo, C. A. *J. Chem. Soc., Dalton Trans.* **2001**, 499. (b) Lu, J. Y.; Cabrera, B. R.; Wang, R.-J.; Li, J. *Inorg. Chem.* **1999**, *38*, 4608. (c) Fokin, S.; Ovcharenko, V.; Romanenko, G.; Ikorskii, V. *Inorg. Chem.* **2004**, *43*, 969.
- (9) (a) MacGillivray, L. R.; Atwood, J. L. *Angew. Chem., Int. Ed.* **1999**, *38*, 1018. (b) Holliday, B. J.; Mirkin, C. A. *Angew. Chem., Int. Ed.* **2001**, *40*, 2022. (c) Lee, J. W.; Samal, S.; Selvapalam, N.; Kim, H.-J.; Kim, K. *Acc. Chem. Res.* **2003**, *36*, 621. (d) Leininger, S.; Olenyuk, B.; Stang, P. J. *Chem. Rev.* **2000**, *100*, 853. (e) Graves, C. R.; Merlau, M. L.; Morris, G. A.; Sun, S.-S.; Nguyen, S. T.; Hupp, J. T. *Inorg. Chem.* **2004**, *43*, 2013. (f) Bera, J. K.; Bacsa, J.; Smucker, B. W.; Dunbar, K. R. *Eur. J. Inorg. Chem.* **2004**, 368. (g) Gianneschi, N. C.; Bertin, P. A.; Nguyen, S. T.; Mirkin, C. A.; Zakharov, L. N.; Rheingold, A. L. *J. Am. Chem. Soc.* **2003**, *125*, 10508.
- (10) Oh, M.; Stern, C. L.; Mirkin, C. A. *Chem. Commun.* **2004**, 2684.
- (11) Hartshorn, C. M.; Steel, P. J. *J. Chem. Soc., Dalton Trans.* **1998**, 3927.

- (12) Frank, W.; Reiland, V.; Reiss, G. *J. Angew. Chem., Int. Ed.* **1998**, *37*, 2984.

groups. This study shows an example of the stoichiometry of the reaction used to control the type of polymer that forms, and it examines the role of several types of aromatic–aromatic interactions (face-to-face, face-to-edge, and inclined) in the formation of these supramolecular systems.

Experimental Section

General Procedures. Unless otherwise noted, all reactions and manipulations were performed under an atmosphere of dry nitrogen using standard Schlenk techniques. All solvents were dried and distilled prior to use according to standard methods.¹³ All deuterated solvents were purchased and used as received from Cambridge Isotopes Laboratories. All other chemicals were obtained from commercial sources and used as received unless otherwise noted. ¹H NMR spectra were obtained using a Varian Gemini 300 MHz FT-NMR spectrometer and referenced relative to tetramethylsilane. Electron ionization mass spectra (EIMS) were recorded on a Fisons VG 70-250 SE mass spectrometer. Electrospray (ES) mass spectra were obtained on a Micromas Quatro II triple quadrupole mass spectrometer. Elemental analyses were obtained from Quantitative Technologies Inc., Whitehouse, NJ.

The ligands L1 and L2 were prepared as previously reported.^{10,11} Formation of these compounds and their purity were verified by comparing their NMR spectra with known spectra.

Synthesis of L3. 4-Mercaptophenol (1.63 g, 12.91 mmol), Cs₂CO₃ (8.83 g, 27.11 mmol), and 2-picolyl chloride hydrochloride (4.45 g, 27.11 mmol) were mixed in CH₃CN (100 mL). The resulting suspension was refluxed for 20 h. After removal of the solvent, the crude product was purified via column chromatography (neutral alumina) with CH₂Cl₂ as an eluent to yield (87%) pure oily product. ¹H NMR (300 MHz, CD₂Cl₂): δ 8.56 (d, 2H), 8.47 (d, 2H), 7.72 (t, 2H), 7.59 (t, 2H), 7.48 (d, 2H), 7.27 (d, 2H), 7.25 (t, 2H), 7.20 (d, 2H), 7.14 (t, 2H), 6.89 (d, 2H), 5.17 (s, 2H), 4.13 (s, 2H). EIMS (*m/z*): calcd for L3, 308.1; found, 308.1.

Synthesis of L4. 4,4'-Biphenol (2.00 g, 10.74 mmol), Cs₂CO₃ (7.35 g, 22.55 mmol), and 2-picolyl chloride hydrochloride (3.70 g, 22.55 mmol) were mixed in CH₃CN (150 mL). The resulting suspension was refluxed for 20 h. After removal of the solvent, the crude product was purified via column chromatography (neutral alumina) with CH₂Cl₂ as an eluent to give pure product in 89% yield. ¹H NMR (300 MHz, CD₂Cl₂): δ 8.59 (d, 2H), 7.75 (t, 2H), 7.55 (d, 2H), 7.49 (d, 4H), 7.27 (t, 2H), 7.04 (d, 4H), 5.23 (s, 4H). EIMS (*m/z*): calcd for L4, 368.2; found, 368.2.

Synthesis of L5. Bis(4-hydroxyphenyl)methane (2.00 g, 9.99 mmol), Cs₂CO₃ (6.84 g, 20.98 mmol), and 2-picolyl chloride hydrochloride (3.44 g, 20.98 mmol) were mixed in CH₃CN (150 mL). The resulting suspension was refluxed for 20 h. After removal of the solvent, the crude product was purified via column chromatography (neutral alumina) with CH₂Cl₂ as an eluent. Solvent was evaporated to give 83% yield of pure product. ¹H NMR (300 MHz, CD₂Cl₂): δ 8.56 (d, 2H), 7.74 (t, 2H), 7.52 (d, 2H), 7.25 (t, 2H), 7.10 (d, 4H), 6.90 (d, 4H), 5.17 (s, 4H), 3.84 (s, 2H). EIMS (*m/z*): calcd for L5, 382.2; found, 382.2.

Synthesis of {[Ag(L2)]CF₃SO₃}_n (1). An acetone solution (2 mL) of L2 (20.0 mg, 0.068 mmol) was added to a solution of AgCF₃SO₃ (17.6 mg, 0.068 mmol) in 2 mL of acetone at room temperature. The resulting solution was slowly evaporated in a vial. After 1 day, crystals of polymer **1** suitable for X-ray diffraction studies were obtained in 77% yield. Anal. Calcd for C₃₈H₃₂Ag₂F₆N₄O₁₀S₂: C, 41.55; H, 2.94; N, 5.10. Found: C, 41.65; H,

2.78; N, 5.05. Single-crystal X-ray analysis was used to determine the solid-state structure of **1**.

Synthesis of {[Ag(L2)]CF₃SO₃}_n (2). An acetone solution (2 mL) of L2 (20.0 mg, 0.068 mmol) was added to a solution of AgCF₃SO₃ (8.8 mg, 0.034 mmol) in 2 mL of acetone at room temperature. The resulting solution was slowly evaporated in a vial. After several hours, crystals of polymer **2** suitable for X-ray diffraction studies were obtained in 85% yield. Anal. Calcd for C₃₇H₃₂AgF₃N₄O₇S: C, 52.80; H, 3.83; N, 6.66. Found: C, 52.53; H, 3.70; N, 6.53. Single-crystal X-ray analysis was used to determine the solid-state structure of **2**.

Synthesis of {[Ag(L4)]CF₃SO₃}_n (3). An acetone solution (2 mL) of L4 (20.0 mg, 0.054 mmol) was added to a solution of AgCF₃SO₃ (13.9 mg, 0.054 mmol) in 2 mL of acetone at room temperature. The resulting solution was slowly evaporated in a vial. After 1 day, crystals of polymer **3** suitable for X-ray diffraction studies were obtained in 71% yield. Anal. Calcd for C₂₅H₂₀AgF₃N₂O₅S: C, 48.02; H, 3.22; N, 4.48. Found: C, 47.88; H, 3.07; N, 4.45. Single-crystal X-ray analysis was used to determine the solid-state structure of **3**.

Synthesis of {[Ag(L5)]CF₃SO₃}_n (4). An acetone solution (2 mL) of L5 (20.0 mg, 0.052 mmol) was added to a solution of AgCF₃SO₃ (13.4 mg, 0.052 mmol) in 2 mL of acetone at room temperature. The resulting solution was slowly evaporated in a vial. After 1 day, crystals of polymer **4** suitable for X-ray diffraction studies were obtained in 68% yield. Anal. Calcd for C₂₆H₂₂AgF₃N₂O₅S: C, 48.84; H, 3.47; N, 4.38. Found: C, 49.02; H, 3.24; N, 4.44. Single-crystal X-ray analysis was used to determine the solid-state structure of **4**.

Synthesis of {[Ag₂(L1)(L2)]·2CF₃SO₃}_n (5). Acetone solutions (2 mL) of L1 (10.0 mg, 0.031 mmol) and L2 (9.1 mg, 0.031 mmol) were added consecutively to a solution of AgCF₃SO₃ (15.9 mg, 0.062 mmol) in 2 mL of acetone at room temperature. The pale yellow solution was reduced in volume, and diethyl ether was added to effect precipitation of a pale yellow powder (89% yield). Pale yellow crystals of polymer **5** suitable for X-ray diffraction studies were grown from the slow diffusion of diethyl ether into a concentrated solution of the complex in nitromethane. Anal. Calcd for C₃₈H₃₂Ag₂F₆N₄O₈S₄: C, 40.37; H, 2.85; N, 4.96; S, 11.34. Found: C, 40.38; H, 2.59; N, 4.86; S, 11.55. Single-crystal X-ray analysis was used to determine the solid-state structure of **5**.

Synthesis of [Ag(L3)]₂·2CF₃SO₃ (6). An acetone solution (2 mL) of L3 (20.0 mg, 0.065 mmol) was added to a solution of AgCF₃SO₃ (16.7 mg, 0.065 mmol) in 1 mL of acetone at room temperature. The pale yellow solution was reduced in volume, and diethyl ether was added to precipitate product as a pale yellow powder (92% yield). Pale yellow crystals of **6** suitable for X-ray diffraction studies were grown from the slow diffusion of diethyl ether into a concentrated solution of complex in nitromethane. ¹H NMR (300 MHz, CD₃OD): δ 8.79 (d, 2H), 8.75 (d, 2H), 8.07 (t, 2H), 7.86 (t, 2H), 7.75 (d, 2H), 7.60 (t, 2H), 7.45 (t, 2H), 7.39 (d, 2H), 7.09 (d, 2H), 6.70 (d, 2H), 5.16 (s, 2H), 4.37 (s, 2H). Anal. Calcd for C₁₉H₁₆AgF₃N₂O₄S₂: C, 40.37; H, 2.85; N, 4.96; S, 11.34. Found: C, 40.18; H, 2.68; N, 4.95; S, 11.83. Single-crystal X-ray analysis was used to determine the solid-state structure of **6**.

X-ray Crystal Structure Determination of 1–6. Diffraction intensity data were collected with Bruker SMART-1000 CCD diffractometers equipped with a graphite-monochromated Mo K α radiation source. The data collected were processed to produce conventional intensity data by the program SAINT-NT (Bruker). The intensity data were corrected for Lorentz and polarization effects. Absorption corrections were applied using the SADABS empirical method. The structures were solved by direct methods,

(13) Armarego, W. L. F.; Perrin, D. D. *Purification of Laboratory Chemicals*; Butterworth-Heinemann: Oxford, U.K., 1996.

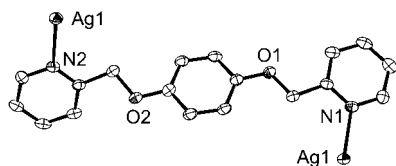


Figure 1. ORTEP representation of a linear conformation of L2 in polymer **1**. Thermal ellipsoids are drawn at 50% probability.

completed by subsequent difference Fourier syntheses, and refined by full matrix least-squares procedures on F^2 . Unless otherwise noted, all the non-hydrogen atoms were refined anisotropically. Hydrogen atoms were added at calculated positions and treated as isotropic contributions. The space groups were chosen on the basis of the systematic absences in the diffraction data. In the structure of **2**, the triflate anion is highly disordered and removed from the diffraction data using the bypass procedure in PLATON.¹⁴ Correction of the X-ray data by SQUEEZE (155 e/cell) was close to the required values (149 e/cell) for the CF_3SO_3 anion. The disordered carbon atoms were refined with isotropic thermal parameters, and the H atoms of the disordered groups were not taken into consideration. All software and sources of scattering factors are contained in the SHELXTL program package (version 5.10, G. Sheldrick, Bruker-AXS, Madison, WI). Crystallographic data for **1–6** are given in Tables 1 and 3.

Results and Discussion

Ligands Synthesis. All of the ligands employed in this study have been synthesized via modified literature procedures.^{10,11} Reaction of 4-mercaptophenol, 4,4'-biphenol, or bis(4-hydroxyphenyl)methane with 2-picoyl chloride hydrochloride in the presence of Cs_2CO_3 in acetonitrile produced bis(2-pyridyl) ligands of L3–L5, respectively (Chart 1). All ligands were purified via column chromatography (neutral alumina) with CH_2Cl_2 as an eluent to yield pure products. The ligands have been characterized by ^1H NMR spectroscopy and mass spectrometry.

Polymers 1–4. The reaction between L2 and AgCF_3SO_3 gives two types of charged polymers (triflate salts), depending upon the ratio of starting materials used (Scheme 2). One polymer, $\{[\text{Ag}(\text{L}2)]\text{CF}_3\text{SO}_3\}_n$ (**1**), which forms from the 1:1 reaction between ligand and metal ion, consists of L2 ligands bridged by silver ions in a linear fashion. The other polymer, $\{[\text{Ag}(\text{L}2)_2]\text{CF}_3\text{SO}_3\}_n$ (**2**), formed from the reaction between 2 equiv of ligand and 1 equiv of metal ion, is a 2D structure with each metal center attached to four L2 ligands. Ligand L2 in polymers **1** and **2** acts as a bis-monodentate ligand with a linear conformation to link two Ag ions (Figures 1 and 2). The nitrate salt of **1** has been reported by others elsewhere,¹¹ and the structure reported herein (Figure 3) only exhibits minor differences in the Ag coordination sphere and Ag–N bond distances. It is used primarily as a comparison for the new structures, **2–6**.

Selected bond distances and angles for **1** are given in Table 2. Each silver center can be regarded as quasi-tetracoordinated with two nitrogen atoms from two distinct ligands and with two triflate oxygen atoms weakly contacted (Figure 3). The Ag–N bond lengths of 2.191 and 2.188 Å are indicative of a bonding interaction,⁶ and the N–Ag–N angle is 159.88°.

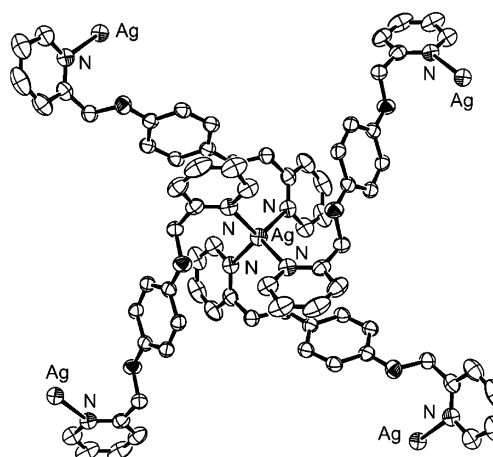
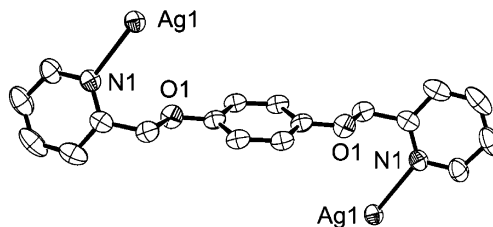


Figure 2. ORTEP representations of a linear conformation of L2 and the coordination environment around Ag(I) in polymer **2**. Thermal ellipsoids are drawn at 50% probability.

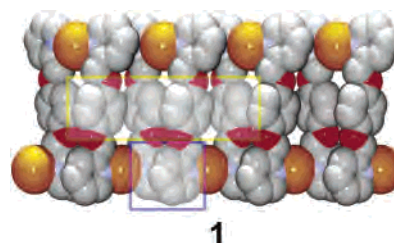


Figure 3. Space-filling representation of the coordination polymer **1**. The boxed area shows aromatic–aromatic interactions between the pyridine groups (blue box, inclined) and the benzene groups (yellow box, face-to-edge). Hydrogen atoms and counterions are omitted for clarity. (Key: Ag, orange; N, light blue; O, red; C, gray.)

The distances between the silver and oxygen atoms of the triflate anion (not shown in Figure 3) are 2.578 and 2.702 Å, which indicates the presence of weak Ag–O interactions.¹⁵ An analysis of the structure suggests that the aromatic–aromatic interactions between L2 ligands are significant and likely contribute to the assembly process and the stabilization of the supramolecular polymeric structures. There are two types of aromatic–aromatic interactions in structure **1**. One is an inclined type^{4f} interaction between the pyridyl groups with the shortest carbon–nitrogen atoms distance of 3.26 Å (Figure 3, blue box), and the other is a face-to-edge⁵ type interaction between the arene groups with a CH–ring distance of 2.67 Å (Figure 3, yellow box).

Each silver center in polymer **2** has a distorted tetrahedral geometry with four nitrogen atoms from four distinct L2 ligands (Figure 2). Selected bond distances and angles for **2** are given in Table 2. The Ag–N bond length of 2.353 Å in

(14) Van der Sluis, P.; Spek, A. L. *Acta Crystallogr.* **1990**, *A46*, 194.

(15) Ino, I.; Zhong, J. C.; Munakata, M.; Kuroda-Sowa, T.; Maekawa, M.; Suenaga, Y.; Kitamori, Y. *Inorg. Chem.* **2000**, *39*, 4273.

Table 1. Crystallographic Data for 1–4

	1	2	3	4
formula	C ₃₈ H ₃₂ Ag ₂ F ₆ N ₄ O ₁₀ S ₂	C ₃₇ H ₃₂ AgF ₃ N ₄ O ₇ S	C ₂₅ H ₂₀ AgF ₃ N ₂ O ₅ S	C ₂₆ H ₂₂ AgF ₃ N ₂ O ₅ S
fw	1098.54	841.60	625.36	639.39
cryst syst	monoclinic	tetragonal	monoclinic	triclinic
space group	<i>P</i> 2 ₁ / <i>c</i>	<i>P</i> 4/ <i>n</i>	<i>P</i> 2 ₁ / <i>c</i>	<i>P</i> $\bar{1}$
<i>a</i> , Å	11.4595(11)	14.5894(11)	14.4669(9)	8.7805(6)
<i>b</i> , Å	8.8258(8)	14.5894(11)	8.8499(5)	17.4841(12)
<i>c</i> , Å	19.7469(19)	8.5601(9)	19.0088(12)	18.6170(12)
α , deg	90	90	90	113.7450(10)
β , deg	93.203(2)	90	102.4980(10)	102.7020(10)
γ , deg	90	90	90	91.0730(10)
<i>V</i> , Å ³	1994.1(3)	1822.0(3)	2376.0(2)	2533.6(3)
<i>Z</i>	2	2	4	4
<i>d</i> _{calcd} , Mg m ⁻³	1.830	1.534	1.748	1.676
μ , mm ⁻¹	1.179	0.680	1.001	0.941
θ range, deg	1.78–28.79	1.97–28.71	1.44–28.93	1.36–29.00
temp, K	153(2)	153(2)	153(2)	153(2)
no. indepnt reflns	4850 (<i>R</i> _{int} = 0.0306)	2245 (<i>R</i> _{int} = 0.0875)	5832 (<i>R</i> _{int} = 0.0387)	11 899 (<i>R</i> _{int} = 0.0325)
no. of params refined	280	102	334	685
<i>R</i> ₁ , <i>wR</i> ₂	0.0335, 0.0782	0.0436, 0.1080	0.0339, 0.0808	0.0370, 0.0902
GOF	1.083	0.961	1.073	1.064

Table 2. Selected Bond Distances and Angles for 1–4^a

Compound 1 ^b			
Ag(1)–N(1)	2.191(2)	Ag(1)–N(2) ^{#1}	2.188(2)
Ag(1)–O(4) ^{#2}	2.578(2)	Ag(1)–O(5)	2.702(2)
N(1)–Ag(1)–N(2) ^{#1}	159.88(8)	N(1)–Ag(1)–O(4) ^{#2}	95.77(8)
N(2) ^{#1} –Ag(1)–O(4) ^{#2}	86.89(8)	N(1)–Ag(1)–O(5)	93.71(8)
N(2) ^{#1} –Ag(1)–O(5)	105.29(8)	O(4) ^{#2} –Ag(1)–O(5)	101.82(7)
Compound 2 ^c			
Ag(1)–N(1)	2.353(2)		
N(1)–Ag(1)–N(1) ^{#1}	121.16(6)	N(1)–Ag(1)–N(1) ^{#2}	88.00(9)
Compound 3 ^d			
Ag(1)–N(1)	2.185(2)	Ag(1)–N(2) ^{#1}	2.194(2)
Ag(1)–O(4) ^{#2}	2.627(2)	Ag(1)–O(5) ^{#3}	2.634(2)
N(1)–Ag(1)–N(2) ^{#1}	156.25(7)	N(1)–Ag(1)–O(4) ^{#2}	94.90(7)
N(2) ^{#1} –Ag(1)–O(4) ^{#2}	85.73(7)	N(1)–Ag(1)–O(5) ^{#3}	97.34(6)
N(2) ^{#1} –Ag(1)–O(5) ^{#3}	105.88(7)	O(4) ^{#2} –Ag(1)–O(5) ^{#3}	100.83(6)
Compound 4 ^e			
Ag(1)–N(3)	2.168(2)	Ag(1)–N(4)	2.159(2)
Ag(1)–O(7)	2.795(2)	Ag(1)–O(9) ^{#1}	2.771(2)
Ag(2)–N(1)	2.188(2)	Ag(2)–N(2)	2.204(2)
Ag(2)–O(6) ^{#2}	2.498(2)	Ag(2)–O(8)	2.590(2)
N(3)–Ag(1)–N(4)	165.70(8)	N(3)–Ag(1)–O(7)	86.70(8)
N(4)–Ag(1)–O(7)	105.68(8)	N(3)–Ag(1)–O(9) ^{#1}	95.96(8)
N(4)–Ag(1)–O(9) ^{#1}	88.23(8)	O(7)–Ag(1)–O(9) ^{#1}	103.29(8)
N(1)–Ag(2)–N(2)	148.45(8)	N(1)–Ag(2)–O(6) ^{#2}	96.70(8)
N(2)–Ag(2)–O(6) ^{#2}	97.08(8)	N(1)–Ag(2)–O(8)	108.85(7)
N(2)–Ag(2)–O(8)	100.18(7)	O(6) ^{#2} –Ag(2)–O(8)	86.63(8)

^a All oxygen atoms mentioned here originate from triflate anions. ^b Symmetry transformations used to generate equivalent atoms: (#1) 1 – *x*, 1/2 + *y*, 3/2 – *z*; (#2) 2 – *x*, 1 – *y*, 2 – *z*. ^c Symmetry transformations used to generate equivalent atoms: (#1) –1/2 + *y*, 1 – *x*, 1 – *z*; (#2) 1/2 – *x*, 3/2 – *y*, *z*. ^d Symmetry transformations used to generate equivalent atoms: (#1) 2 – *x*, –1/2 + *y*, 3/2 – *z*; (#2) 2 – *x*, –*y*, 1 – *z*; (#3) 1 + *x*, *y*, *z*. ^e Symmetry transformations used to generate equivalent atoms: (#1) –1 + *x*, *y*, –1 + *z*; (#2) 1 + *x*, *y*, 1 + *z*.

2 is somewhat longer than in polymer **1**, and the N–Ag–N angles are 88.00 and 121.16°. Polymer **2** forms a 2D network possessing pores with approximate dimensions of 6 Å × 6 Å (Figure 4). These 2D porous networks are stacked along the *c*-axis to give open channels.¹⁶ A three-layer π – π stacking interaction between three distinct ligands with a

ring–ring distance of 3.48 Å seems to stabilize the 2D networks (Figure 4, blue box).

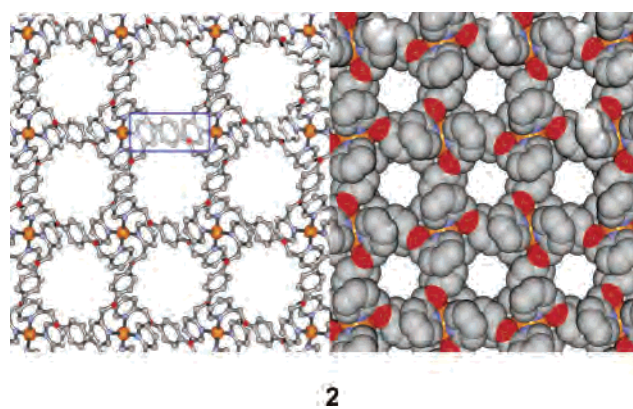


Figure 4. Ball-and-stick and space-filling representations of the coordination polymer **2**. The boxed area shows the close contact between the pyridine groups and the central arene groups, consistent with strong π – π stacking interactions. Hydrogen atoms and counterions are omitted for clarity. (Key: Ag, orange; N, light blue; O, red; C, gray.)

The reactions of L4 and L5 with silver ions in a 1:1 metal-to-ligand ratio also yield 1D polymers with structures that are similar to that of polymer **1** (Scheme 2). Slow evaporation of mixtures of the ligands (L4 or L5) and AgCF₃SO₃ afforded colorless single crystals of the one-dimensional polymers {[Ag(L4)]CF₃SO₃}_{*n*} (**3**) and {[Ag(L5)]CF₃SO₃}_{*n*} (**4**). Crystallographic data, selected bond distances, and angles for **3** and **4** are given in Tables 1 and 2. Ligands L4 and L5 in polymers **3** and **4** exhibit similar modes of bonding to the Ag⁺ ions (Figure 5). They act as bis-monodentate ligands linking two silver ions through nitrogen atoms. Each silver center can be described as quasi-tetracoordinated with two nitrogen atoms from two distinct ligands and weak contacts from two triflate oxygen atoms, as in polymer **1**. The range of Ag–N bond lengths (2.185–2.194 Å (**3**), 2.159–2.204 Å (**4**)) indicates a bonding interaction,⁶ and the range of Ag–O bond lengths from 2.498 to 2.795 Å is indicative of the presence of relatively weaker Ag–O interactions.¹⁵ The N–Ag–N angles are 156.25° for polymer **3** and 165.70 and 148.46° for polymer **4**. The distortion of the N–Ag–N bond

(16) (a) Biradha, K.; Hongo, Y.; Fujita, M. *Angew. Chem., Int. Ed.* **2002**, *41*, 3395. (b) Zou, R.-Q.; Bu, X.-H.; Zhang, R.-H. *Inorg. Chem.* **2004**, *43*, 5382. (c) Lu, J. Y.; Babb, A. M. *Chem. Commun.* **2003**, 1346. (d) Ko, J. W.; Min, K. S.; Suh, M. P. *Inorg. Chem.* **2002**, *41*, 2151.

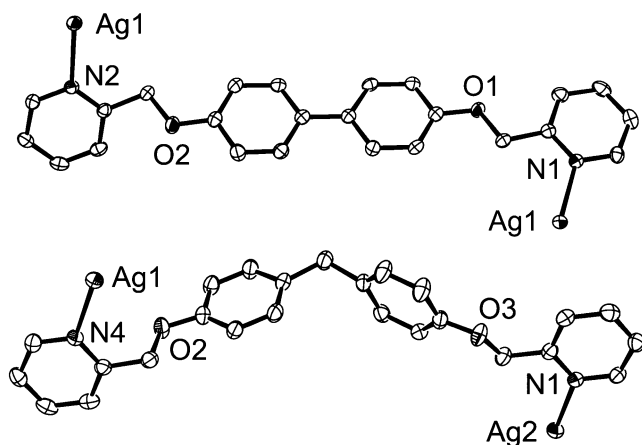


Figure 5. ORTEP representations of linear conformations of L4 and L5 in polymers **3** and **4**. Thermal ellipsoids are drawn at 50% probability.

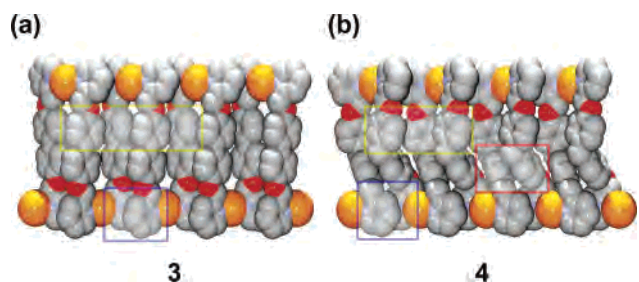


Figure 6. Space-filling representations of the coordination polymers (a) **3** and (b) **4**. The boxed area shows aromatic–aromatic interactions between the pyridine groups (blue box, inclined) and the benzene groups (yellow box, face-to-edge and red box, face-to-face). Hydrogen atoms and counterions are omitted for clarity. (Key: Ag, orange; N, light blue; O, red; C, gray.)

angles from linearity is caused by the interaction of the triflate anion with the silver ion.

The aromatic–aromatic interactions in polymers **3** and **4** seem to play an important role in stabilizing the polymeric structures (Figure 6). In the case of polymer **3**, there are inclined aromatic–aromatic interactions between pyridyl groups with the shortest carbon–nitrogen atoms distance being 3.33 Å (Figure 6a, blue box) and face-to-edge CH– π interactions with a CH–ring distance of 2.78 Å (Figure 6a, yellow box). The X-ray structure of polymer **4** shows three types of aromatic–aromatic interactions: inclined interactions between the pyridyl groups with the shortest carbon–nitrogen atoms distance being 3.25 Å (Figure 6b, blue box); face-to-face interactions between the arene rings with a ring–ring distance of 3.55 Å (Figure 6b, red box); face-to-edge interactions between the arene rings with a CH–ring distance of 2.91 Å (Figure 6b, yellow box).

Polymer 5 and Macrocycle 6. In general, pyridin-2-ylmethoxy ligands, L2, L4, and L5 (Chart 1), act as bis-monodentate ligands coordinating to silver ions through the nitrogen atoms only. However, the (pyridin-2-yl-methyl)-thio ligand, L1, typically acts as a bis-bidentate ligand where both the nitrogen and sulfur atoms interact with silver ions.¹⁰ Ligand L1, in previously studied complex $\{[\text{Ag}(\text{L1})]\text{CF}_3\text{SO}_3\}_n$, adopts a folded conformation with the pyridine moieties pointed away from the central arene linker and toward one another.¹⁰ We investigated the reaction of silver ions in the presence of two different ligands, L1 and L2,

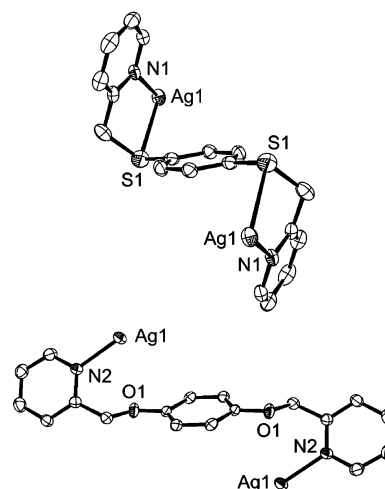


Figure 7. ORTEP representations of a folded conformation of L1 and a linear conformation of L2 in polymer **5**. Thermal ellipsoids are drawn at 50% probability.

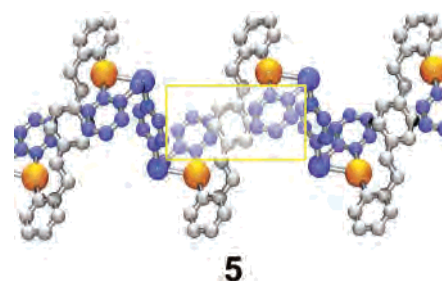


Figure 8. Ball-and-stick representation of the coordination polymer **5**. The boxed area shows the face-to-edge CH– π interaction between the pyridine groups of L1 and the central arene of L2. Hydrogen atoms and counterions are omitted for clarity. (Key: Ag, orange; L1, blue; L2, gray.)

in a 1:1 ratio. Interestingly, a one-dimensional polymer $\{[\text{Ag}_2(\text{L1})(\text{L2})]\cdot 2\text{CF}_3\text{SO}_3\}_n$ (**5**) was obtained by the reaction of AgCF_3SO_3 with 0.5 equiv of L1 followed by the reaction with 0.5 equiv of L2 in acetone at room temperature (Scheme 3, left). Pale yellow single crystals were grown by slow diffusion of diethyl ether into a concentrated nitromethane solution of the complex. An interesting feature of the reaction is the formation of an alternative ABAB type coordination copolymer rather than the homopolymers $\{[\text{Ag}(\text{L1})]\text{CF}_3\text{SO}_3\}_n$ and $\{[\text{Ag}(\text{L2})]\text{CF}_3\text{SO}_3\}_n$. Copolymers¹² consisting of two similarly functionalized components are rare in coordination chemistry.

Single-crystal X-ray analysis of polymer **5** reveals that the asymmetric unit consists of one Ag center, half of L1, and half of L2 (Figure 7). As one would expect, L1 acts as a bis-bidentate ligand, adopting a folded conformation with the pyridine moieties pointed away from the central arene linker and away from one another, and L2 acts as a bis-monodentate ligand with a linear conformation. The silver metal ions are coordinated in a highly distorted tetrahedral geometry to two nitrogen atoms, one from L1 and one from L2, one sulfur atom from L1, and one oxygen atom from the triflate anion (Figure 8). Crystallographic data, selected bond distances, and angles for **5** are given in Tables 3 and 4. The Ag–N distances are 2.181 and 2.174 Å, indicative of a bonding interaction. In contrast, there are comparatively weak bonding interactions between the silver and sulfur

Table 3. Crystallographic Data for **5** and **6**

	5	6
formula	C ₃₈ H ₃₂ Ag ₂ F ₆ N ₄ O ₈ S ₄	C ₂₁ H ₂₁ AgF ₃ N ₂ O _{4.5} S ₂
fw	1130.66	602.39
cryst syst	triclinic	triclinic
space group	<i>P</i> $\bar{1}$	<i>P</i> $\bar{1}$
<i>a</i> , Å	9.0500(6)	8.563(3)
<i>b</i> , Å	10.7333(7)	9.015(3)
<i>c</i> , Å	11.3373(7)	16.064(5)
α , deg	91.4810(10)	86.167(5)
β , deg	94.7020(10)	83.847(5)
γ , deg	111.9030(10)	71.745(4)
<i>V</i> , Å ³	1016.43(11)	1170.1(6)
<i>Z</i>	1	2
<i>d</i> _{calcd} , Mg m ⁻³	1.847	1.710
μ , mm ⁻¹	1.255	1.097
θ range, deg	1.81–28.73	1.28–28.88
temp, K	153(2)	153(2)
no. indpdnt reflns	4752 (<i>R</i> _{int} = 0.0179)	5517 (<i>R</i> _{int} = 0.0425)
no. params refined	280	314
<i>R</i> 1, <i>wR</i> 2	0.0389, 0.1047	0.0431, 0.1242
GOF	1.028	1.039

Table 4. Selected Bond Distances and Angles for **5** and **6**^a

Compound 5 ^b			
Ag(1)–N(1)	2.180(3)	Ag(1)–N(2)	2.174(3)
Ag(1)–S(1)	2.786(1)	Ag(1)–O(2) ^{#1}	2.696(3)
N(1)–Ag(1)–N(2)	169.30(10)	N(1)–Ag(1)–S(1)	77.33(7)
N(2)–Ag(1)–S(1)	113.01(7)	N(1)–Ag(1)–O(2) ^{#1}	94.76(11)
N(2)–Ag(1)–O(2) ^{#1}	89.02(11)	S(1)–Ag(1)–O(2) ^{#1}	85.28(6)
Compound 6 ^c			
Ag(1)–N(1)	2.308(3)	Ag(1)–N(2) ^{#1}	2.177(3)
Ag(1)–S(1)	2.552(1)	Ag(1)–O(4)	2.585(3)
N(1)–Ag(1)–N(2) ^{#1}	125.57(11)	N(1)–Ag(1)–S(1)	79.66(8)
N(2) ^{#1} –Ag(1)–S(1)	152.99(8)	N(1)–Ag(1)–O(4)	98.63(11)
N(2) ^{#1} –Ag(1)–O(4)	92.80(10)	S(1)–Ag(1)–O(4)	92.37(8)

^a All oxygen atoms mentioned here originate from triflate anions.

^b Symmetry transformations used to generate equivalent atoms: (#1) *x*, 1 + *y*, *z*. ^c Symmetry transformations used to generate equivalent atoms: (#1) 1 – *x*, 1 – *y*, 1 – *z*.

atoms and the silver and oxygen atoms as evidenced by the bond distances of 2.786 and 2.696 Å, respectively.

The reaction of L3, which has both (pyridin-2-yl-methyl)-thio (NS) and pyridin-2-ylmethoxy (NO) groups, with silver triflate results in the formation of a 20-membered bimetallic macrocycle [Ag₂(L3)₂]·2CF₃SO₃ (**6**) rather than a polymeric structure (Figure 9). Ligand L3 adopts a half-folded conformation in the macrocycle where the nitrogen atom in the NO portion coordinates to the silver atom and the NS portion interacts with the silver atom through both the nitrogen and sulfur atoms. In this cyclic unit, the Ag–Ag distance is 9.67 Å. Two pyridine groups and one sulfur atom are coordinated to each Ag ion. The triflate counterion (not shown in Figure 9) is also weakly coordinated through an oxygen atom making the coordination geometry capped trigonal planar. The Ag–N(1) bond length of 2.308 Å is slightly longer than the Ag–N(2) bond length of 2.177 Å. The Ag–S bond length of 2.552 Å is shorter than that observed in **5**, so the N–Ag–N angle of 125.57° is more distorted from the linear coordination geometry observed in **5** (169.30°). The ¹H NMR spectrum of **6** shows resonances for the pyridyl and methylthio units shifted downfield due to their coordination to the silver metal, while the signals associated with the methoxy unit resemble those of the free ligand (see Experi-

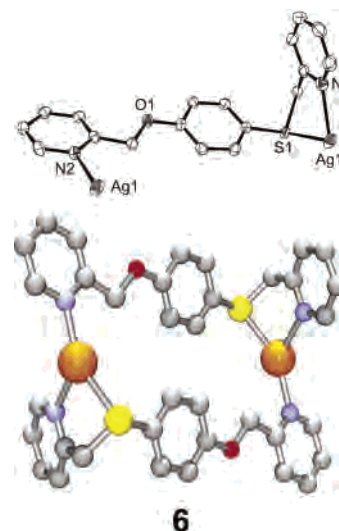


Figure 9. ORTEP representation of half-folded conformation of L3 in macrocycle **6** with thermal ellipsoids at 50% probability and ball-and-stick representation of the macrocycle. Hydrogen atoms and counterions are omitted for clarity. (Key: Ag, orange; N, light blue; S, yellow; O, red; C, gray.)

mental Section). Unlike the polymeric species, there are no significant aromatic–aromatic interactions in the dimeric macrocycle.

Conclusions

This work describes the formation of Ag(I) coordination polymers and a macrocycle based on flexible bis(2-pyridyl) ligands (L1–L5). The pyridine group is only coordinated to silver in the NO portions with a linear conformation while the NS portions act as bidentate ligands where both nitrogen and sulfur atoms interact with silver ions in a folded conformation. Reactions of 1 equiv of L2, L4, or L5 with silver ions give 1D chain coordination polymers (**1**, **3**, and **4**). In contrast to this, a stoichiometric change to a 2:1 L2-to-silver ion ratio results in the formation of a 2D porous network (**2**). This work also demonstrates a rare example of an ABAB coordination copolymer (**5**) generated from the combination of L1 and L2 with silver ions. An investigation of the structures reveals that all five polymeric structures possess significant aromatic–aromatic interactions, which likely stabilize and guide the formation of such structures. In contrast to this, the reaction of L3 with silver ions gives a bimetallic macrocycle (**6**) rather than polymeric species. The geometry of L3 makes it difficult to form polymeric species, and no significant aromatic–aromatic interactions are observed in the solid-state structure of the macrocycle.

Acknowledgment. C.A.M. acknowledges the National Science Foundation and Air Force Office of Scientific Research for generous financial support.

Supporting Information Available: X-ray crystallographic files in CIF format. This material is available free of charge via the Internet at <http://pubs.acs.org>.

IC0482990